Differential cross section for the $^2H(\gamma,p)n$ reaction between 100 and 255 MeV

E. De Sanctis,[a] M. Anghinolfi,[b] G. P. Capitani,[a] P. Corvisiero,[b] P. Di Giacomo,[a]
C. Guaraldo,[a] V. Lucherini,[a] E. Polli,[a] A. R. Reolon,[a]
G. Ricco,[b] M. Sanzone,[b] and A. Zucchiatti[b]

[a]*Istituto Nazionale di Fisica Nucleare—Laboratori Nazionali di Frascati, I-00044 Frascati, Italy*

[b]*Dipartimento di Fisica dell'Università di Genova and Istituto Nazionale di Fisica Nucleare-Sezione di Genova, I 16146 Genova, Italy*

(Received 16 December 1985)

Differential cross sections for the $^2H(\gamma,p)n$ reaction were measured at five laboratory angles from 32.5° to 130°, for photon energies between 100 and 255 MeV, in 10 MeV steps. A quasi-monochromatic photon beam, obtained by positron in-flight annihilation on a liquid hydrogen radiator, was used, and the photon spectrum was measured on-line by a pair spectrometer. The normalization uncertainty is within ±5%. Data agree, within the total errors, with recent results of a tagged-photon experiment and of a measurement of the inverse process. The measured angular distributions were fitted by a sum of Legendre polynomials, and the results compared with recent calculations. Significant departures from the calculated angular distribution asymmetry have been found.

I. INTRODUCTION

The photodisintegration of the deuteron has been fairly extensively studied both by experimentalists and theoretists, because this process can provide basic information on the properties of nuclear forces, the effects of intrinsic degrees of freedom of a nucleon on nuclear properties, and possible exotic multiquark excited states (dibaryon resonances). Nevertheless, in spite of the considerable effort spent so far on these studies, the knowledge of the deuteron photodisintegration cross section is still unsatisfactory. This is in particular true in the energy region between the pion emission threshold and the $\Delta(1232)$ resonance, where the spread of experimental values[1–12] covers a factor of 2 in the absolute normalization, well outside the quoted error limits. On the theoretical side, in this energy region where meson exchange currents and isobar phenomena make relevant contributions, several approaches[13–18] are able to describe the general features of the cross section, but still differ from each other. Of course, due to the large discrepancy existing among experiments, a reliable comparison between theory and experiment has not yet been possible.[19]

Recently, the development of new techniques for producing monochromatic photon beams and of advanced computational capabilities has pushed the $^2H(\gamma,p)n$ reaction into the forefront of renewed experimental and theoretical interest.

In this paper we report the results of a new experiment on the deuteron photodisintegration process at intermediate energies performed in view of the need for more reliable data. A preliminary account of this experiment was recently published.[20] Well aware that the large discrepancies in the experimental data are not removed by the simple addition of yet another data set, we have designed the experiment with primary attention to the minimization of systematic uncertainties. We have taken advantage of the availability at Frascati of a quasi-monochromatic photon beam, which, though not strictly necessary for the measurement of a two-body reaction, obviously offers important advantages, making it possible to check unambiguously both proton detector energy calibration and response function. Moreover, particular care was taken with the monitoring of the positron and photon beams, as described below.

In Sec. II we describe the experimental procedure and in Sec. III the data analysis and corrections. A discussion of our results and a comparison with data from other recent experiments and with theoretical prediction is contained in Sec. IV. The consequences of this measurement with respect to various theoretical approaches are outlined in Sec. V followed by conclusions in Sec. VI.

II. EXPERIMENTAL PROCEDURE

The measurement was carried out using the LEALE (Laboratorio Esperienze Acceleratore Lineare Elettroni) quasi-monochromatic photon beam produced at Frascati by in-flight positron annihilation.[21] The layout of the experimental apparatus is schematically shown in Fig. 1. Positrons left the beam pipe through an aluminum win-

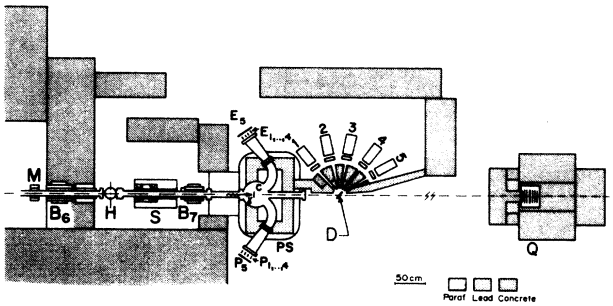

FIG. 1. The experimental setup for the $^2H(\gamma,p)n$ reaction study: M, ferrite toroid monitor; B_6, deflecting magnet; B_7, sweeping magnet; H, liquid hydrogen target; S, dumping magnet; PS, pair spectrometer, with the relevant converter C and the associated electron (E_i) and positron (P_i) detection system; D, liquid deuterium target; 1–5 E-ΔE, telescopes; Q, quantameter.

dow and annihilated on a 0.0118 radiation-length thick liquid hydrogen radiator, H. The intensity of the positron beam was continuously monitored by a nonintercepting ferrite toroid, M, and measured by a Faraday cup (also used as beam catcher), placed in the focal plane of a dumping magnet, S.

Of course, in addition to monochromatic annihilation photons, bremsstrahlung is also produced. In order to reduce the relative bremsstrahlung-to-annihilation contribution, measurements were carried out by collecting photons at 0.7°—0.9° with respect to the positrons. The selection of the angle was achieved by a two-magnet system, which changed the incident positron angle, leaving the photon axis unchanged.

The photon beam was collected within a solid angle of 0.048 msr, defined by a lead collimator inserted in the yoke of the dumping magnet. The next dipole magnet B_7 swept off from the beam any residual charged particles. A rectangular flat pole C-type magnet, PS, was used as an on-line pair spectrometer. Photons entered the magnetic field region through a hole opened in the yoke of the magnet and were converted into an (e^-e^+) pair by a remotely selectable aluminum converter. The used converter was thin enough (3.37×10^{-4} radiation lengths) to produce a small accidental-to-true events ratio in spite of the poor machine duty factor (10—30 nA average current, 150 Hz repetition rate, ~4 μs beam burst duration). Therefore also the beam attenuation and the loss of efficiency due to multiple scattering and energy losses in the converter were negligible. In order to reduce background production from air, the beam channel was kept under vacuum from the annihilation radiator up to the pair spectrometer exit window.

Electrons and positrons, after a $\sim110°$ deflection by the spectrometer magnet, left the vacuum chamber through a Mylar window 0.125 mm thick, and were detected, along the focal line, by two identical arrays of four counters ($E_1,\ldots,E_4$ and $P_1,\ldots,P_4$) followed by a fifth backing counter (E_5,P_5).

For each setting of the magnetic field the spectrometer defined 16 energy channels which were grouped into seven independent energy bins. Full details on the optical properties of the magnet, the calculation of the response function, and the spectrometer performance are given in Ref. 22.

The integrated photon flux on the deuterium target was finally measured by a Gaussian quantameter,[23] which provided a constant sensitivity in our energy range. The intensity used was typically $\sim5\times10^6$ annihilation photons per second.

The deuterium target consisted of a vertical Mylar cylinder (4.0 cm diameter, wall thickness 0.08 mm), filled with liquid deuterium by a two-stage refrigerator (Cryodine helium refrigerator model 360) installed directly on

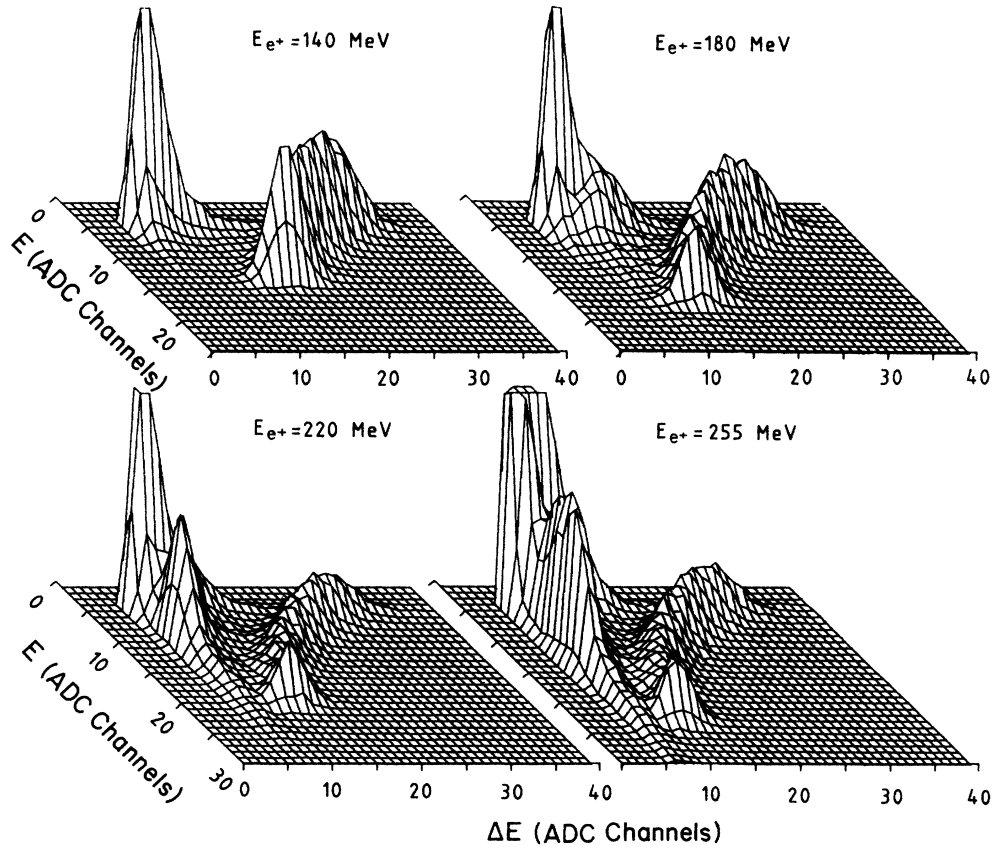

FIG. 2. ΔE vs E plot for the proton telescope set at 105° in the laboratory and for the given positron energies E_{e+}. The small ΔE—small E peak is due to electrons, the shoulder growing on this peak as the positron energy increases is due to pions, and the ridge on the right is due to protons. The electron peak contribution is truncated for scale reasons.

the deuterium cell. A series of thermoresistors, placed in the cell and inside the refrigerator, monitored the level of liquid deuterium and ensured the automatic operation of the system. By continuously monitoring the deuterium vapor pressure we were able to keep the liquid deuterium density constant within $\pm 1\%$.

The photon beam spot on the target had a circular shape of 3.8 cm diameter and was periodically measured with a beam profile monitor.[24] The target vacuum chamber entrance and exit windows, of 4.4×10^{-3} mm Mylar sheet, were located at a distance from the deuterium cell sufficient to prevent a direct line of sight between the windows and any detector.

Charged particles from the target were detected in five dual scintillator telescopes[25] connected on line to a PDP 15/76 computer. The solid angle for each detector, defined by two accurately machined collimators, was equal to about 7 msr. The front counter—a 3 mm thick Ne 102A scintillator—gave a measurement of the energy loss ΔE. In order to ensure good homogeneity and optical efficiency the scintillator was coupled to two Philips 56 AVP type photomultipliers by means of six-sector light pipes. The back counter—a 10.4 cm diam and 12 cm deep NaI crystal coupled to a Philips XP2041 phototube—gave a measurement of the total energy E. The anode pulses from the XP2041 were shaped with a 50 ns and 50 Ω delay line, allowing high counting rates with negligible pile up.

The gain stability of each telescope was checked on-line every 5 min by a green LED (HLMP-3950) positioned at the edge of each scintillator.[26] In the plastic scintillator the optical contact was achieved by a small Lucite light guide, while in the NaI crystal good light collection was obtained by placing the LED inside a cylindrical hole carved into the edge of the Lucite interface necessary to couple the XP2041 phototube to the flat crystal surface. The LED's were triggered by a pair of pulses whose amplitudes were adjusted to correspond to proton energies of 50 and 100 MeV in the NaI detector. This procedure afforded the correction of possible long term instabilities. No instabilities were found which significantly affected the photoproton pulse-height spectra obtained.

The stored data were presented on line as a ΔE vs E plot and the mass discrimination was found to be sufficiently good to distinguish unambiguously protons from other particles. A contamination of less than 10% was found only at high positron energies (220 and 255 MeV) and has been properly accounted for in the off-line analysis. Figure 2 displays, as an example, these plots for the 105° telescope at four positron energies. As shown, the telescope performance allows a clean discrimination between protons and other particles in the whole energy range.

In order to correct for the presence of background protons from (γ,p) reactions in the target walls and windows, measurements were made with and without liquid deuterium in the target cell. The average contribution of these background sources turned out to be $\leq 5\%$.

Proton spectra were recorded at six annihilation photon energies (100, 120, 140, 180, 220, and 255 MeV) and simultaneously at five laboratory angles: 32.5°, 55°, 80°, 105°, and 130° with respect to the photon beam. The measurements were made in several runs distributed over two years and the data from each run were separately analyzed and compared. This provided a check for systematic errors arising from factors in the experimental conditions which might have varied from run to run. The results of different runs were consistent within $\pm 5\%$.

III. DATA ANALYSIS AND CORRECTIONS

Figure 3(a) shows a typical photon energy spectrum measured on line at the given positron energy, E_{e+}, and photon collection angle 0.9°. The histogram represents the result of a Monte Carlo simulation [program PHOCA (Ref. 27)] which also reproduces the photon total energy measured by the quantameter. The excellent agreement between the computed and the measured spectra was obtained by slightly adjusting only the values of two input quantities (positron emittance and photon collection angle) by amounts within the experimental errors.

Figure 3(b) shows the proton energy spectrum measured simultaneously by the 105° telescope. The proton peak, due to the annihilation photon contribution, is clearly evident, showing the remarkable data quality given by the

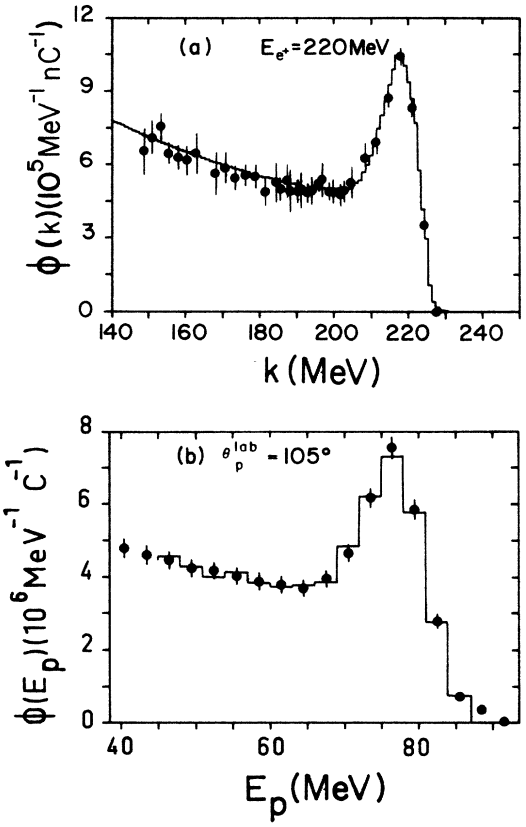

FIG. 3. (a) Photon energy spectrum measured with the pair spectrometer (positron energy 220 MeV, photon collection angle 0.9°, and half angular geometric photon acceptance 3.9 mr). The histogram is a result of a Monte Carlo calculation. (b) Proton energy spectrum measured with the telescope set at $\theta_p^{lab}=105°$ in the laboratory. The histogram is a result of a Monte Carlo calculation.

use of a quasi-monochromatic photon beam. Similar spectra were obtained for all the positron energies and proton angles. Because of the kinematics of the reaction, the proton energy, at any given angle, is uniquely defined by the energy of the incident photon producing the reaction. Therefore the positions and shapes of proton peaks are uniquely related to the relevant annihilation photon peaks, provided that factors such as kinematics and proton energy loss in the target and materials between target and detectors are taken into account. Figure 4 shows the relationship between pulse height analyzer channel and proton peak energy for each telescope: the observed linear dependence provided a check of the linearity of the proton detector system.

A Monte Carlo program (TARGET) has been used to account for the effects to finite photon beam and extended target geometry on the proton detectors. The program simulated the experimental photoproton spectra including, for each event, all the corrections such as actual solid angle, multiple scattering and energy losses in the target and scintillators, rescattering by the collimators, nuclear absorption, and edge effects in the NaI detectors. Input data were the measured photon spectrum, the complete geometry of the apparatus, and a trial photodisintegration cross section which was iterated until the simulated spectrum became compatible, within statistical errors, with the measured proton energy distribution. The final iteration gave the corrected experimental photodisintegration cross section with its uncertainty. A reliable consistency test of this procedure was provided by the fitting of the peak shapes, which were almost completely determined by target thickness and geometry effects, the intrinsic energy resolution of the telescopes (2—3 %) (Ref. 25) being much smaller than the observed peak width. In Fig. 3(b) the histogram is the result of this Monte Carlo simulation: As shown, the agreement between the computed and the measured spectra is excellent.

At first, only the peaks in the photon and proton spectra were used to determine the cross sections. Subsequently, by means of the TARGET program, it has been possible to determine the cross section also by using the bremsstrahlung tail region. Particular care has been taken in selecting the minimum energy values of the proton spectra to be used for this determination in order to be certain that protons from processes in which pions are produced were not being counted. This procedure allowed a cross check on the consistency of cross sections obtained at different positron beam energies: Good agreement was found between values obtained from the annihilation peaks and those from the bremsstrahlung tails. As an example, in Fig. 5 are plotted the c.m. cross sections obtained at $\theta_p^{lab}=105°$, from different energy positron beams. As shown, the agreement between different measurements is always satisfactory.

IV. EXPERIMENTAL RESULTS

The center-of-mass cross sections obtained from the six positron energy measurements were sorted into 10 MeV wide photon energy bins and combined to form one data set. The resulting cross sections as a function of photon energy for the five telescopes are plotted in Fig. 6 and listed in Table I. The errors quoted are statistical only and do not include a ±5% systematic uncertainty on the absolute values of the cross section.

In Fig. 7 our angular distributions (solid dots) are compared with the results of other recent measurements, specifically the neutron radiative-capture experiment by Meyer *et al.*,[28] and three photodisintegration experiments: the tagged-photon study by Arends *et al.*[12] and the

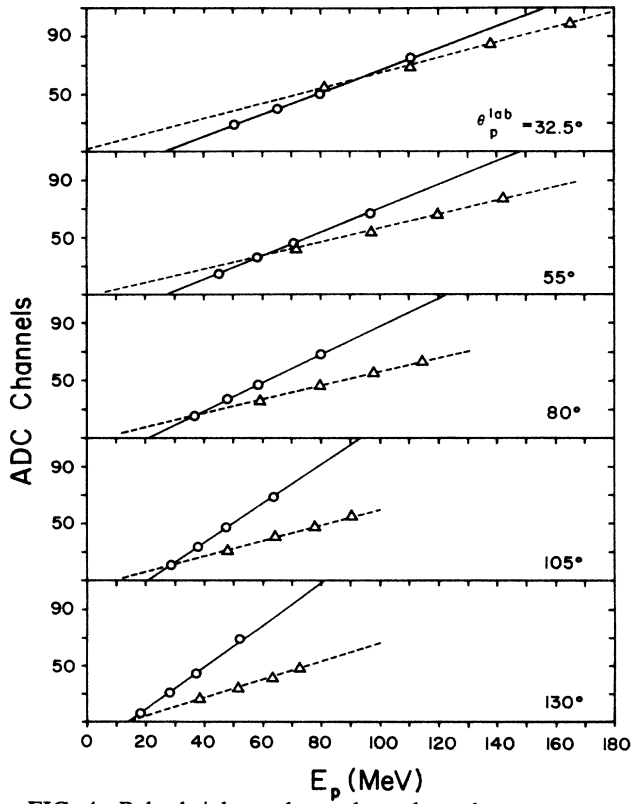

FIG. 4. Pulse height analyzer channel number vs proton energy for the five proton telescopes. Two gain settings have been used for positron energies ≤180 MeV (open circles) and ≥180 MeV (open triangles), respectively.

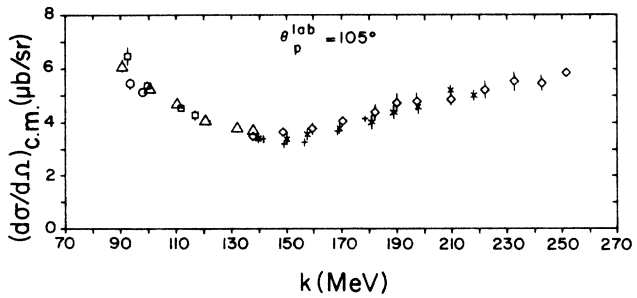

FIG. 5. $^2H(\gamma,p)n$ differential cross section values obtained at $\theta_p^{lab}=105°$ from different energy positron beams: 255 MeV (◇), 220 MeV (*), 180 MeV (+), 140 MeV (△), 120 MeV (□), and 100 MeV (○).

bremsstrahlung experiments by Hughes *et al.*[10] at 0° and by Althoff *et al.*[29] at 180°. In particular, the data of Meyer *et al.*[28] are found to be in agreement with our results within their experimental errors, which include systematic contributions except for the uncertainty on the nucleon-nucleon cross section. The tagged-photon data[12] include only statistical errors; when we take into account their ±4% and our ±5% systematic uncertainties, the two measurements are compatible.

It is therefore definitely encouraging that the new data obtained by using "monochromatic" photons (annihilation or tagged photons) are found to be in agreement within the quoted total errors. There is also agreement with a measurement of the inverse reaction, and consequently a reasonable basis of experimental values is provided for comparison with the theory.

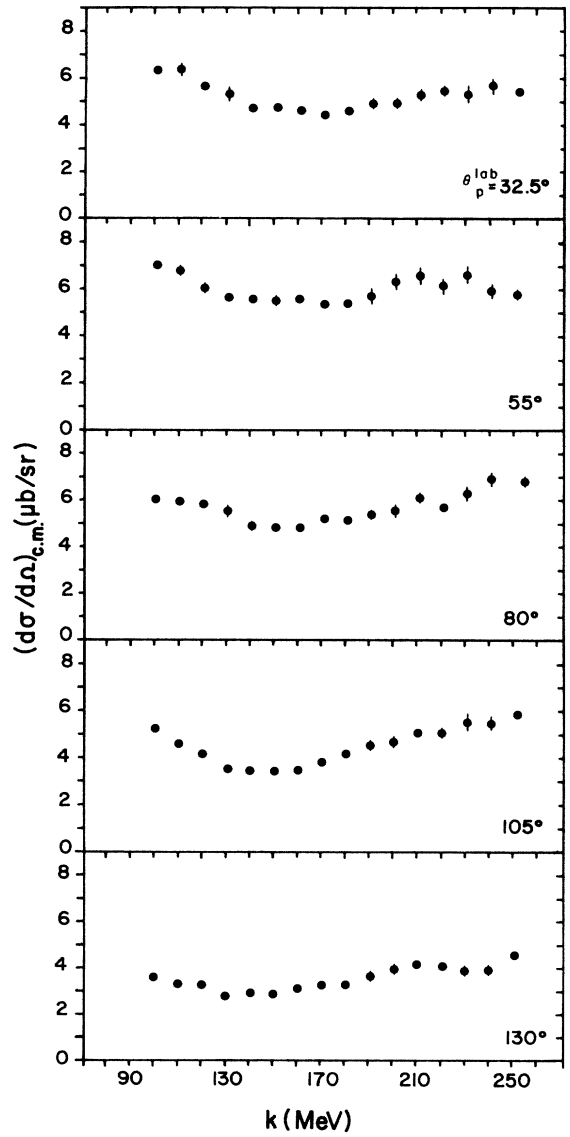

FIG. 6. Measured differential cross sections for the $^2H(\gamma,p)n$ process as a function of the photon energy for the given proton angles in the laboratory.

Moreover, it may be worthwhile to note that our data in the 100–140 MeV range are compatible with the fit obtained by De Pascale *et al.*[30] from a critical review of all the $^2H(\gamma,p)n$ data in the 6–140 MeV range, published before 1982 (dashed curve in Fig. 7).

In Fig. 8 our data at $k=100$, 140, 180, and 220 MeV are compared with the most recent calculations: the dashed curves result from a calculation performed by Laget[15] using an expansion of the photodisintegration amplitude in terms of dominant diagrams. Final state interactions are taken into account by including neutron-proton rescattering in S and P waves. In this calculation Laget has used the values $\Lambda_\pi=1.2$ GeV for the cutoff mass of the pion-baryon form factor, and $G_\rho^2/G_\pi^2=1.6$ for the ratio between the squares of the ρ- and π-baryon coupling constants.

The dotted-dashed curves are a result from Leidemann and Arenhövel,[16] who have extended their low energy calculation beyond the pion photoproduction threshold using the Argonne V_{28} potential with explicit Δ degrees of freedom in the impulse approximation and a coupled channel treatment including all final states interactions and multipole expansion up to $L=4$.

The solid curve are a calculation from Cambi, Mosconi, and Ricci,[17] who have studied the effect of higher order

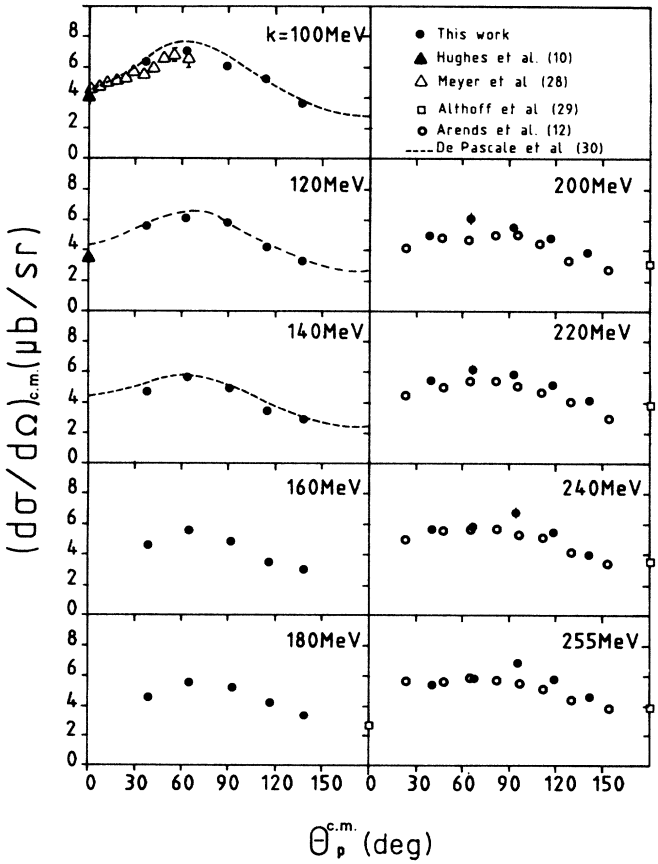

FIG. 7. Comparison among recent angular distribution measurements for the $^2H(\gamma,p)n$ process. Our data and those of Ref. 12 do not include systematic errors (±5% and ±4%, respectively).

TABLE I. Measured values of the c.m. differential cross section for $^2H(\gamma,p)n$ process. The errors are statistical only. Uncertainty in absolute normalization is ±5%.

k (MeV)	$\theta_p^{lab}=32.5°$	$\theta_p^{lab}=55°$	$\theta_p^{lab}=80°$	$\theta_p^{lab}=105°$	$\theta_p^{lab}=130°$
100	6.32±0.14	7.02±0.10	6.03±0.09	5.25±0.08	3.62±0.09
110	6.36±0.23	6.82±0.17	5.97±0.15	4.61±0.11	3.30±0.06
120	5.65±0.14	6.07±0.18	5.83±0.11	4.19±0.11	3.28±0.08
130	5.33±0.30	5.67±0.13	5.56±0.24	3.42±0.08	2.79±0.06
140	4.73±0.12	5.58±0.15	4.92±0.09	3.47±0.08	2.91±0.06
150	4.77±0.13	5.51±0.17	4.86±0.12	3.45±0.10	2.88±0.09
160	4.62±0.15	5.59±0.17	4.85±0.12	3.50±0.12	3.05±0.10
170	4.44±0.14	5.37±0.18	5.22±0.12	3.84±0.09	3.27±0.11
180	4.58±0.12	5.46±0.20	5.16±0.11	4.18±0.10	3.28±0.12
190	4.94±0.19	5.72±0.31	5.39±0.18	4.56±0.20	3.63±0.18
200	4.97±0.21	6.21±0.34	5.55±0.28	4.77±0.19	3.96±0.19
210	5.29±0.21	6.58±0.37	6.11±0.19	5.08±0.14	4.20±0.17
220	5.45±0.23	6.16±0.34	5.84±0.21	5.09±0.18	4.11±0.16
230	5.34±0.37	6.63±0.37	6.32±0.32	5.56±0.36	3.89±0.21
240	5.69±0.31	5.92±0.31	6.79±0.30	5.50±0.31	3.93±0.21
250	5.41±0.16	5.78±0.18	6.80±0.17	5.87±0.15	4.58±0.15

contributions to the one-body (Darwin-Foldy and spin orbit terms plus relativistic corrections to the wave functions) and to the two-body (one-pion-exchange both in pseudoscalar and pseudovector coupling) charge densities.

The solid curves give a better agreement with the experimental points, particularly at $k=100$ MeV, and this shows the importance of contributions from relativistic corrections. The other two curves are systematically higher at forward and backward angles, the discrepancy increasing with photon energy. This is probably related to the strength of the intermediate-range isovector tensor force, which seems to be too large.[16] Moreover, Fig. 8 shows that, with increasing energy above 140 MeV, the measured differential cross sections near 90° become increasingly larger than the theoretical values.

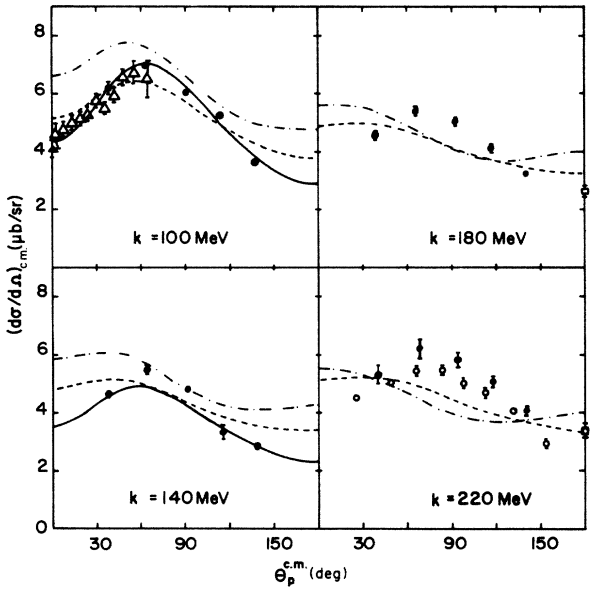

FIG. 8. $^2H(\gamma,p)n$ differential cross section values for the given photon energies. Our data (solid dots) are compared to most recent experimental results and theoretical predictions: open triangles, Ref. 28; closed triangles, Ref. 10; open circles, Ref. 12; open squares, Ref. 29; dashed line, Ref. 15; dotted-dashed line, Ref. 16; solid line, Ref. 17. Our points and those of Ref. 12 do not include systematic errors (±5% and ±4%, respectively).

V. DISCUSSION

The previous statement on the relative consistency, within the quoted total errors, of experimental data on the deuteron photodisintegration reaction obtained by "monochromatic" photons is valid also at energies higher than 255 MeV for the tagged-photon experiments of Arends *et al.*[12] and Baba *et al.*[11] Consequently, the "monochromatic" photon experiments provide a reliable set of data for comparison with the theory. In the present section, therefore, we present the result obtained by fitting by a sum of Legendre polynomials,

$$(d\sigma/d\theta)_{c.m.}=\sum_L A_L P_L(\cos\theta)\ ,$$

the angular dependence of the differential cross section in the energy range from 100 to 440 MeV from our measurement and from Refs. 10–12. The data are well described by the sum with $L_{max}=3$. The numerical values of the coefficients so obtained are listed in Table II and plotted, as a function of the photon energy, in Fig. 9. The error bars result from the least-squares fitting procedure and include the relative fluctuation of different data sets. The obtained fit confirms the consistency of the total cross section values ($4\pi A_0$) from recent deuteron photodisintegration experiments within a ±5% uncertainty.

For the sake of completeness, in Fig. 9 are also plotted the values of the coefficients obtained, for photon energies ≤100 MeV, by De Pascale *et al.*[30] from a fit to all earlier measurements.

Figure 9 also shows the values of the coefficients de-

duced by fitting the theoretical angular distributions calculated by Laget[15] (dashed curve), by Leidemann and Arenhövel[16] (dotted-dashed curve), and by Cambi, Mosconi, and Ricci[17] (solid line curve). The comparison between experiments and calculations supports, on a more general basis, the previous conclusions. The total cross section $4\pi A_0$, as well the interference coefficients A_1 and A_3, are reasonably well reproduced, while $-A_2$ is strongly underestimated at energies greater than 80 MeV. The coefficient A_3 cannot be determined as accurately as the other parameters. Considering the error bars, the experimental values of A_3 appear in reasonable agreement with calculation.

The coefficient A_2 determines the curvature of the an-

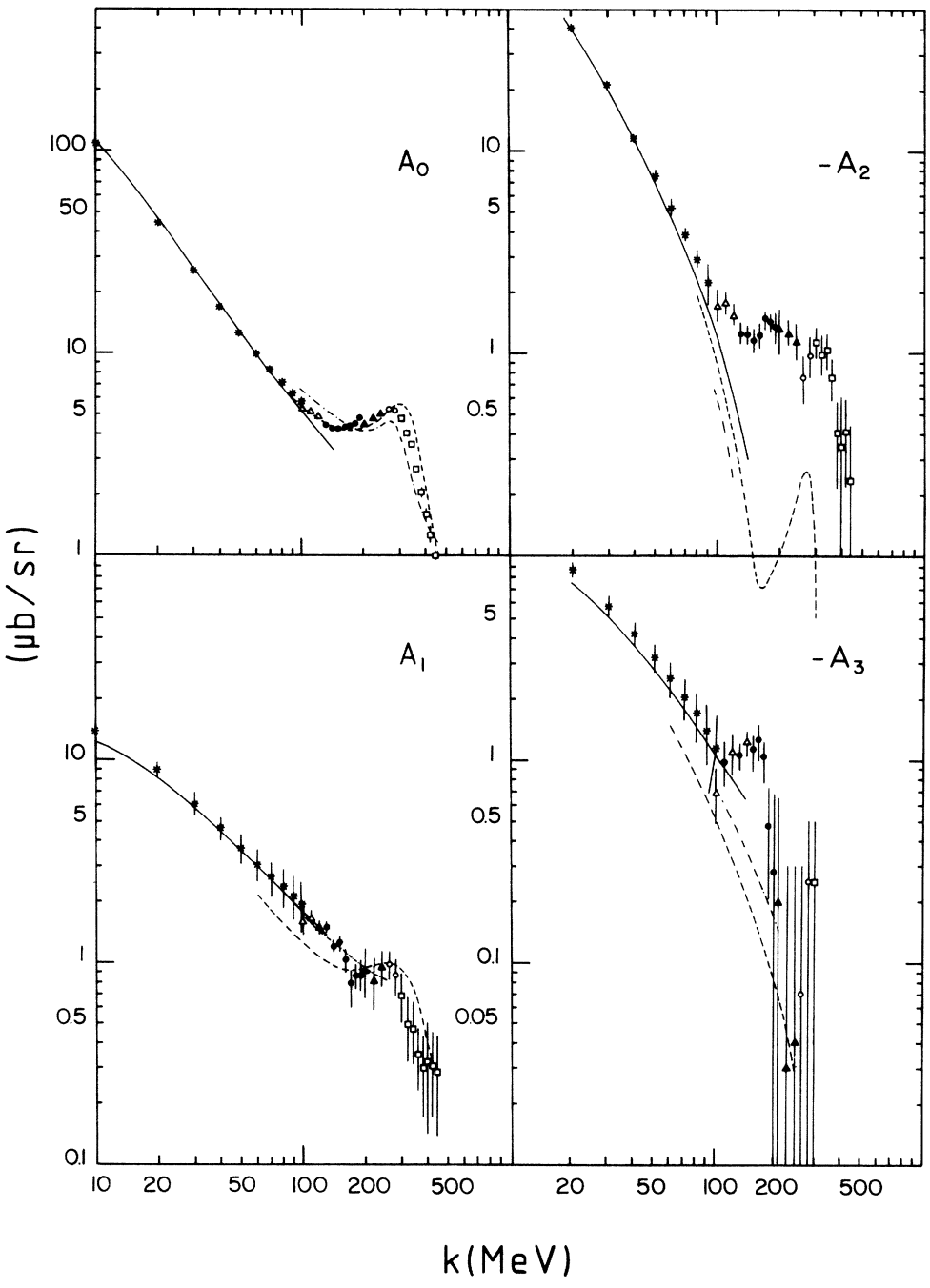

FIG. 9. Obtained results for the Legendre coefficients A_i ($i=0,\ldots,3$) as a function of photon energy: open triangles, present results plus data from Refs. 10 and 28 (only at $k=100$ MeV); solid circles, present results only; solid triangles, present results plus Ref. 12 data; open circles, data from Ref. 12 only; open squares, data from Refs. 11 and 12; asterisks, data from Ref. 30; dashed, dotted-dashed, and solid lines are from Refs. 15, 16, and 17, respectively.

TABLE II. Fitted values for the coefficients A_i ($i=0,1,2,3$).

k (MeV)	A_0 (μb/sr)	A_1 (μb/sr)	A_2 (μb/sr)	A_3 (μb/sr)	Expt. data
100	5.48±0.14	1.61±0.26	−1.74±0.31	−0.69±0.23	a,b,c
110	5.26±0.09	1.68±0.12	−1.78±0.20	−0.98±0.24	a,b
120	4.95±0.08	1.50±0.11	−1.55±0.17	−1.09±0.24	a,b
130	4.43±0.05	1.49±0.07	−1.24±0.15	−1.06±0.15	a
140	4.31±0.04	1.20±0.07	−1.23±0.11	−1.25±0.15	a
150	4.29±0.06	1.24±0.10	−1.17±0.14	−1.12±0.24	a
160	4.33±0.06	1.02±0.12	−1.23±0.15	−1.26±0.25	a
170	4.41±0.09	0.78±0.18	−1.50±0.15	−1.02±0.24	a
180	4.52±0.06	0.86±0.12	−1.46±0.15	−0.47±0.26	a
190	4.81±0.09	0.87±0.15	−1.38±0.24	−0.28±0.41	a
200	4.52±0.14	0.92±0.25	−1.32±0.34	−0.20±0.45	a,d
220	4.79±0.12	0.83±0.25	−1.28±0.17	−0.03±0.30	a,d
240	5.03±0.10	0.95±0.18	−1.15±0.24	−0.04±0.30	a,d
260	5.24±0.10	0.98±0.16	−0.76±0.20	−0.07±0.30	d
280	5.17±0.09	0.86±0.18	−0.97±0.21	−0.25±0.30	d
300	4.76±0.12	0.68±0.18	−1.14±0.20	−0.25±0.30	d,e
320	4.09±0.10	0.49±0.17	−0.99±0.22		d,e
340	3.54±0.10	0.47±0.16	−1.04±0.21		d,e
360	2.69±0.09	0.35±0.12	−0.76±0.18		d,e
380	2.05±0.09	0.30±0.13	−0.41±0.18		d,e
400	1.60±0.10	0.32±0.18	−0.35±0.26		d,e
420	1.27±0.09	0.31±0.14	−0.41±0.19		d,e
440	1.01±0.09	0.29±0.15	−0.24±0.20		d,e

[a]Present work.
[b]Reference 10.
[c]Reference 28.
[d]Reference 12.
[e]Reference 11.

gular distribution around 90°. Present results indicate that, above 80 MeV, $-A_2$ has a greater value (smaller isotropic component) than predicted by theory. According to Arenhövel,[31] the anomalous high cross section in the forward and backward direction around 300 MeV originates from the normal (i.e., without isobar effects) contribution, which is dominated by the $E1$ amplitudes and their interference terms, the resonant $M1$ amplitude being almost isotropic. We may therefore expect that the inclusion of relativistic corrections and/or a weaker tensor term, which already improved the agreement at forward angles below the π production threshold, may also reduce the observed discrepancy in the Δ excitation region.

VI. CONCLUSIONS

A quasi-monochromatic photon beam has been used to measure differential cross sections for the deuteron photodisintegration process between 100 and 255 MeV, over the angular range of 32.5°—130°. The simultaneous determination of both photon energy and photon flux, respectively, by a pair spectrometer and a Gaussian quantameter, made an accurate measurement of the cross section possible. The total normalization uncertainty is within ±5%.

It has been shown that there is an agreement, within the total errors, among measurements of the ^{2}H(γ,p)n differential cross section performed by using quasi-monochromatic photons and tagged photons. The data also agree with results from a recent measurement of the inverse process.

Recent theoretical calculations reproduce the main features of the data, but are not yet able to quantitatively describe the energy and angular dependences of the differential cross sections over the full measured domain. In particular, they predict more isotropic angular distributions than those observed.

ACKNOWLEDGMENTS

We acknowledge the linac operation crew for their cooperation, and the LEALE and Genova technical staffs for their assistance during the data-taking phase of the experiment. We thank Dr. J. M. Laget, Dr. H. Arenhövel, Dr. W. Leidemann, Dr. A. Cambi, Dr. B. Mosconi, and Dr. M. Ricci for making available a version of their calculations in the kinematical conditions of our experiment.

[1]J. C. Keck and A. V. Tollestrup, Phys. Rev. **101**, 360 (1956).
[2]E. A. Whalin, B. D. Schriever, and A. O. Hanson, Phys. Rev. **101**, 377 (1956).
[3]A. Alexandrov, N. B. Delone, L. I. Slovokhotov, G. A. Sokol, and L. N. Shtarkov, Zh. Eksp. Teor. Fiz. **33**, 614 (1957) [Sov. Phys.—JETP **6**, 472 (1958)].
[4]R. Kose, W. Paul, K. Stockhorts, and K. H. Kissler, Z. Phys. **202**, 364 (1967).
[5]A. M. Smith, S. J. Hall, B. Mann, and D. T. Stewart, J. Phys. A (Proc. Phys. Soc.) Ser. 2, Vol. 1, p. 553 (1968).
[6]J. Buon, V. Gracco, J. Lefrancois, P. Lehmann, B. Merkel, and Ph. Roy, Phys. Lett. **26B**, 595 (1968).
[7]D. I. Sober, D. G. Cassel, A. J. Sadoff, K. W. Chen, and P. A. Crean, Phys. Rev. Lett. **22**, 430 (1969).
[8]R. L. Anderson, R. Prepost, and B. H. Wiik, Phys. Rev. Lett. **22**, 651 (1969).
[9]P. Dougan, T. Kvikas, K. Lugner, V. Ramsay, and W. Stiefler, Z. Phys. A **276**, 55 (1976); P. Dougan, V. Ramsay, and W. Stiefler, *ibid.* **280**, 341 (1977).
[10]R. J. Hughes, Z. Zieger, H. Waffler, and B. Ziegler, Nucl. Phys. **A267**, 329 (1976).
[11]K. Baba, I. Endo, H. Fukuma, K. Inoue, T. Kawamoto, T. Ohsugi, Y. Sumi, T. Takeshita, S. Uehara, Y. Yano, and T. Maki, Phys. Rev. Lett. **48**, 729 (1982); Phys. Rev. C **28**, 286 (1983).
[12]J. Arends, H. J. Gassen, A. Hegerath, B. Mecking, G. Noldeke, P. Prenzel, T. Reichelt, A. Voswinkel, and W. W. Sapp, Nucl. Phys. **A412**, 509 (1981).
[13]K. Ogawa, T. Kamae, and K. Nakamura, Nucl. Phys. **A340**, 451 (1980).
[14]M. Anastasio and M. Chemtob, Nucl. Phys. **A364**, 219 (1981).
[15]J. M. Laget, Nucl. Phys. **A312**, 265 (1978); Can. J. Phys. **62**, 1046 (1984), and private communication.
[16]W. Leidemann and H. Arenhövel, Phys. Lett. **139B**, 22 (1984); Can. J. Phys. **62**, 1036 (1984), and private communication.
[17]A. Cambi, B. Mosconi, and M. Ricci, Phys. Rev. C **26**, 2358 (1982); J. Phys. G **10**, L11 (1984), and private communication.
[18]W. Y. P. Hwang, J. T. Londergan, and G. E. Walker, Ann. Phys. (N.Y.) **149**, 335 (1983).
[19]M. Sanzone, Frascati Report No. LNF-83/66(R), 1983.
[20]E. De Sanctis, G. P. Capitani, P. Di Giacomo, C. Guaraldo, V. Lucherini, E. Polli, A. R. Reolon, R. Scrimaglio, M. Anghinolfi, P. Corvisiero, G. Ricco, M. Sanzone, and A. Zucchiatti, Phys. Rev. Lett. **54**, 1639 (1985).
[21]G. P. Capitani, E. De Sanctis, P. Di Giacomo, C. Guaraldo, V. Lucherini, E. Polli, A. R. Reolon, R. Scrimaglio, M. Anghinolfi, P. Corvisiero, G. Ricco, M. Sanzone, and A. Zucchiatti, Nucl. Instrum. Methods **216**, 307 (1983).
[22]G. P. Capitani, E. De Sanctis, P. Di Giacomo, C. Guaraldo, V. Lucherini, E. Polli, A. R. Reolon, and R. Scrimaglio, Nucl. Instrum. Methods **178**, 61 (1980).
[23]A. P. Komar, S. P. Kruglov, and I. V. Lopatin, Nucl. Instrum. Methods **82**, 125 (1970).
[24]M. Albicocco, G. P. Capitani, E. De Sanctis, P. Di Giacomo, C. Guaraldo, V. Lucherini, E. Polli, and A. R. Reolon, Nucl. Instrum. Methods **203**, 63 (1982).
[25]A. Zucchiatti, M. Sanzone, and E. Durante, Nucl. Instrum. Methods **129**, 467 (1975).
[26]M. Anghinolfi, M. Castoldi, M. Albicocco, and E. Polli, Nuovo Cimento **88A**, 257 (1985).
[27]G. P. Capitani, E. De Sanctis, P. Di Giacomo, C. Guaraldo, V. Lucherini, E. Polli, A. R. Reolon, and V. Bellini, Nucl. Instrum. Methods **203**, 353 (1982); E. De Sanctis, V. Lucherini, and V. Bellini, Comput. Phys. Commun. **30**, 71 (1983).
[28]H. O. Meyer, J. R. Hall, M. Hugi, H. J. Karwowski, R. E. Pollock, and P. Schwandt, Phys. Rev. Lett. **52**, 1759 (1984); Phys. Rev. C **31**, 309 (1985).
[29]K. H. Altoff, G. Anton, D. Bour, B. Bock, W. Ferber, and H. W. Gelhausen, N. Horikawa, Th. Jahnen, O. Kaul, W. Konig, K. C. Konigsmann, D. Menze, W. Meyer, Th. Miczaika, E. Roderburg, and W. Ruhm, Z. Phys. C **21**, 149 (1983).
[30]M. P. De Pascale, G. Giordano, P. Picozza, L. Azario, R. Caloi, L. Casano, L. Ingrosso, M. Mattioli, E. Poldi, D. Prosperi, and C. Schaerf, Phys. Lett. **119B**, 30 (1982).
[31]H. Arenhövel, in *Electron and Photon Interactions at Intermediate Energies,* Vol. 234 of *Lecture Notes in Physics,* edited by D. Menze, W. Pfeil, and W. J. Schwille (Springer-Verlag, Berlin, 1984), p. 276.

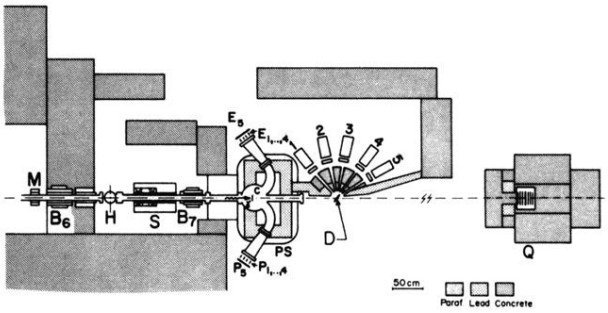

FIG. 1. The experimental setup for the ^{2}H(γ,p)n reaction study: M, ferrite toroid monitor; B_6, deflecting magnet; B_7, sweeping magnet; H, liquid hydrogen target; S, dumping magnet; PS, pair spectrometer, with the relevant converter C and the associated electron (E_i) and positron (P_i) detection system; D, liquid deuterium target; 1—5 E-ΔE, telescopes; Q, quantameter.